Status on Testing of JENDL-3.3 with Shielding Benchmarks

Naoki YAMANO*†
* *Shielding Integral Test Working Group, Japanese Nuclear Data Committee*
† *Department of Nuclear Design, Sumitomo Atomic Energy Industries, Ltd.*
2-10-14 Ryogoku, Sumida-ku, Tokyo 130-0026
e-mail: yamano@sae.co.jp

Integral test of neutron and gamma-ray production data for the latest version of Japanese Evaluated Nuclear Data Library, Version 3.3 (JENDL-3.3) has been performed by using shielding benchmarks. An evaluation scheme for shielding benchmark analyses established in Japanese Nuclear Data Committee is applied to the integral test for Sodium, Titanium, Vanadium, Chromium, Iron, Nickel, Niobium and Tungsten. Calculations are made based on a continuous-energy Monte Carlo code MCNP4B/4C, and deterministic multi-group codes ANISN and DORT. The latest version of NJOY99 is employed to generate cross-section libraries for these transport codes. The status of the integral test activity is reviewed, and some benchmark results for medium-heavy nuclei are presented.

1. Introduction

The latest version of Japanese Evaluated Nuclear Data Library, Version 3.3 (JENDL-3.3) is the final stage of evaluation. Japanese Nuclear Data Committee (JNDC) is responsible for accuracy of the evaluation and showing applicability on shielding applications. Shielding Integral Test Working Group (WG) in JNDC has charge of validation work for JENDL-3.3 through shielding benchmark tests. An evaluation scheme [(1)] for shielding benchmark analyses established in JNDC has been applied to the integral tests for medium-heavy nuclei such as Aluminum, Sodium, Titanium, Vanadium, Chromium, Iron, Cobalt, Nickel, Copper, Niobium and Tungsten. In the present study, some benchmark results of neutron and gamma-ray production data are shown for Sodium, Iron, Vanadium, Tungsten, Nickel, Titanium, Niobium and Chromium.

2. Evaluation Scheme

For the integral test of cross sections by using shielding benchmarks, we should select appropriate integral measurements of different types, that are generally characterized as having good geometry, well-description of experimental method and result, and high sensitivity to the nuclear data of interest. In the present study, we selected a number of spectrum measurements listed in Table 1 to derive a general conclusion for energy-dependent data accuracy. For calculation, two comprehensive systems should be applied based on different approximations between cross-section processing and transport methods to evaluate errors due to each calculation process. We used a continuous-energy Monte Carlo code MCNP4B/4C,[(2)] and multi-group discrete ordinates codes ANISN [(3)] and DORT.[(4)] The latest version of NJOY99 [(5)] was employed to generate cross-section libraries for these transport codes. Then, a systematic analysis procedure was introduced to specify the accuracy and definite problems for typical reactions of nuclear data when discrepancy was found between calculation result and measurement. Calculations with JENDL-3.2,[(6)] JENDL-FF,[(7)] ENDF/B-VI,[(8)] FENDL-1 [(9)] and FENDL-2 [(10)] were also made for comparison.

3. Results and Discussions

3.1 Sodium

SDT4 benchmark called the Broomstick experiment, which was performed to investigate the effect of minima in the neutron total cross sections in the MeV energy range was analyzed. The results for 60.56 cm thick sodium are shown in Fig. 1.

---

* C. Ichihara, K. Ueki, Y. Matsumoto, F. Maekawa, C. Konno, Y. Hoshiai, K. Sasaki, M. Takemura, S. Suzuki, M. Kawai and A. Hasegawa

The neutron spectrum calculated with JENDL-3.3 showed a good agreement with experiment, and it was comparable to that of JENDL-3.2 except below 1 MeV. The difference is not a problem, since the absolute fluxes are relatively small in the energy region. Figures 2 and 3 show the results of JASPER IVFS-IC/Pb.9 (197.4 cm thick sodium) and JASPER IHX-IB/Pb (231.3 cm thick sodium) configurations, respectively. The results with JENDL-3.3 indicated a good agreement with both measurements, while these results showed slightly larger than those of JENDL-3.2 in the energy range below 1.5 MeV. The differences are within calculation errors and the same order of the experimental errors.

3.2 Iron

For relatively thin neutron transmission benchmarks, we selected KfK and NIST-ROSPEC experiments from iron spheres with a ^{252}Cf source in the center. Two calculations with ANISN and MCNP4B were employed in the KfK benchmark. The result is shown in Fig. 4 for the KfK iron sphere of 35 cm in diameter. Neutron spectra calculated by using two codes agreed with each other except for resonance minima below 300 keV, but good agreement was obtained between calculation and experiment. Figure 5 shows the result of the NIST-ROSPEC iron sphere of 50.7 cm in diameter. The result with JENDL-3.3 was comparable to that with JENDL-3.2. However, JENDL-3.3 indicated slightly smaller than that with ENDF/B-VI and measurement in the energy range between 2 and 5 MeV in the NIST benchmark, while the tendency did not appear in the KfK configuration. In this energy region, experimental error is relatively large compared with another energy range, and the shape of the source spectrum of ^{252}Cf much affects the calculated result, so that we cannot infer which evaluation is appropriate.

For relatively thick neutron transmission benchmarks, we adopted WINFRITH-ASPIS and JAERI-FNS experiments. Figures 6 and 7 show comparisons between calculated results with MCNP4C and the ASPIS measurements at 85.41 and 113.98 cm-depth in iron slabs, respectively. Figures 8 and 9 indicate comparisons between calculated results with MCNP4C and the FNS measurement at 81 cm-depth in large iron cylinder. In these benchmarks, neutron fluxes calculated with JENDL-3.3 in the energy range between 0.7 and 1 MeV were slightly underestimated compared with experiments. On the contrary, calculations with ENDF/B-VI were much better in this energy region. Two calculation methods with DORT and MCNP4C showed the same flux profile, so that we recommended improvement should be made in the energy range.

For lower energy region below the 24 keV s-wave resonance, we analyzed the FNS benchmark as shown in Fig. 9. JENDL-3.3 slightly showed overestimation compared with experiment. The calculation to experimental (C/E) ratio integrated over between 1 and 1000 eV was relatively large for JENDL-3.3, while the C/E deviations with JENDL-3.3 at each measured position were relatively smaller than those with another libraries.

For gamma-ray production benchmarks, we employed KfK and JAERI-FNS measurements. The results with JENDL-3.3 indicated good agreement with measurements as shown in Figs. 10 through 12, and improvement was generally obtained compared with JENDL-3.2.

3.3 Vanadium

We analyzed neutron and gamma-ray production benchmarks of JAERI-FNS experiments. In Fig. 13, neutron fluxes calculated with JENDL-3.3 showed underestimation below 1 keV, while some improvements were obtained compared with JENDL-3.2. In the energy region above 20 keV, a good agreement was generally obtained except for between 0.1 and 1 MeV. For gamma-ray production data, improvement from JENDL-3.2 was generally obtained as shown in Fig. 14.

3.4 Tungsten

For Tungsten benchmarks, JAERI-FNS and OKTAVIAN measurements were adopted. In Fig. 15, neutron spectrum above 100 keV was slightly underestimated compared with the FNS experiment. For leakage gamma-ray measurements of FNS and OKTAVIAN, photon spectrum profile was generally acceptable but improvement was still required in the energy range above 1 MeV as shown in Figs. 16 through 18.

3.5 Nickel, Titanium, Niobium and Chromium

Figure 19 shows the comparison between calculation with MCNP4C and measurement for the IPPE Nickel sphere experiment. The result was generally acceptable, and no problem was found. For Titanium, comparison of calculated neutron fluxes with ANISN and MCNP4B was shown in Fig. 20 together with the OKTAVIAN measurement. Two calculation methods indicated the same spectrum profile, and overestimation was shown below 3 MeV. Gamma-ray flux calculated with JENDL-3.3 was overestimated in the energy range between 2 and 5 MeV as shown in Fig. 21. Comparisons between calculation and the OKTAVIAN measurement for Niobium and Chromium are shown in Figs. 22 and 23, respectively. Two calculations with ANSIN and MCNP4B showed the same flux profile. Chromium was generally acceptable, however Niobium indicated overestimation below 1 MeV.

4. Conclusion

Integral tests based on various shielding benchmarks were performed for Sodium, Iron, Vanadium, Tungsten, Nickel, Titanium, Niobium and Chromium for JENDL-3.3. The results were generally satisfactory and the new evaluation would be acceptable for shielding applications. However, some recommendations were given, and improvements should be made before official release of JENDL-3.3. A number of calculation results are being frequently informed to the Medium-Heavy Nuclide Data Evaluation WG of JNDC to assess data accuracy and consistency for their evaluation, so that the results in the present study may be changed hereafter until JENDL-3.3 is officially released scheduled in 2001.

Acknowledgments

Authors are indebted to M. Wada of Startcom Co. Ltd. and T. Nishio of Osaka University for their information concerning calculations of the FNS benchmarks. The work was performed as an activity of the Shielding Integral Test WG of JNDC.

References

(1) Yamano, N.: Ann. Nucl. Energy, **24**, 1085 (1997).
(2) Briesmeister, J.F. (ed.): "MCNP-A General Monte Carlo N-Particle Transport Code, Version 4C," LA-13709-M (2000).
(3) Engle Jr., W.W.: "A USER'S MANUAL FOR ANISN: A One Dimensional Discrete Ordinates Transport Code with Anisotropic Scattering," K-1693 (1967).
(4) Rhodes, W.A. and Mynatt, F.R.: Nucl. Sci. Eng., **99**, 88 (1988).
(5) MacFarlane, R.E. and Muir, D.W.: "The NJOY Nuclear Data Processing System, Version 91," LA-12740-M (1994).
(6) Nakagawa, T., et al.: J. Nucl. Sci. Technol., **32**, 1259 (1995).
(7) Chiba, S., et al.: "Evaluation of the Double-Differential Cross Sections of Medium-Heavy Nuclei for JENDL Fusion File," Proc. 3rd Specialists' Meeting on Nuclear Data for Fusion Reactors, Nov. 29-30, 1995, Tokai, Japan, JAERI-Conf 96-005, pp.45-54 (1996).
(8) Rose, P.F. (ed.): "ENDF-201 ENDF/B-VI Summary Documentation," BNL-NCS-17541 (1991).
(9) Ganesan, S. and McLaughin, P.K.: "FENDL/E Evaluated Nuclear Data Library of Neutron Nuclear Interaction Cross-Sections and Photon Production Cross-Sections and Photon-Atom Interaction Cross Sections for Fusion Applications Version 1.0 of May 1994," IAEA-NDS-128 (1995).
(10) Pashchenko, A.B., et al.: "FENDL-2: An Improved Nuclear Data Library for Fusion Applications," Proc. Int. Conf. on Nuclear Data for Science and Technology, May 19-24, Trieste, Italy, 1150 (1997 Italian Physical Society, Vol. 59, Part II).

Table 1 Candidates for Shielding Benchmark Test of JENDL-3.3

Nuclide	Benchmark Experiments
Sodium	SDT4, SDT12, JASPER(IVFS-IC/Pb.9, IHX-IB/Pb)
Aluminum	OKTAVIAN
Silicon	OKTAVIAN
Titanium	OKTAVIAN
Vanadium	FNS
Chromium	OKTAVIAN
Iron	SDT1, FNS, ASPIS, KfK, IPPE, NIST
Cobalt-59	OKTAVIAN
Nickel (include SS316)	IPPE, ORNL, FNS
Copper	OKTAVIAN, FNS
Niobium	OKTAVIAN
Tungsten	OKTAVIAN, FNS

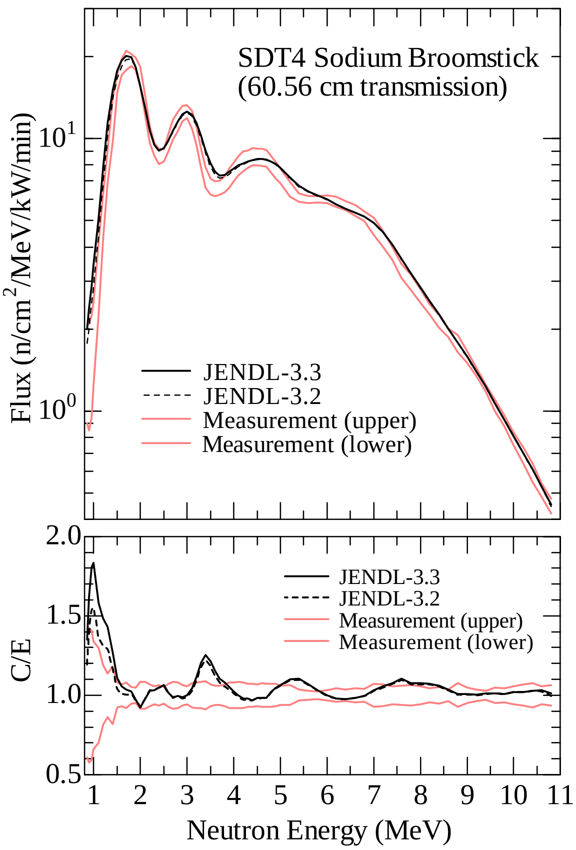

Fig. 1 Results of SDT4 Sodium benchmark.

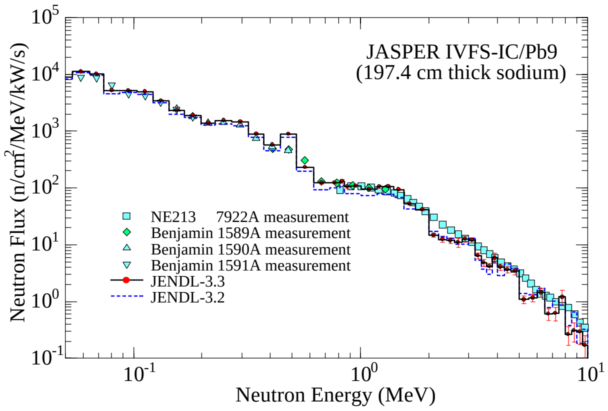

Fig. 2 Results of JASPER IVFS-IC/Pb benchmark.

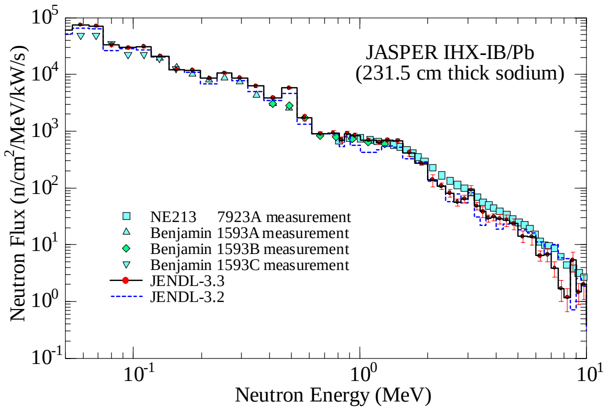

Fig. 3 Results of JASPER IHX-IB/Pb benchmark.

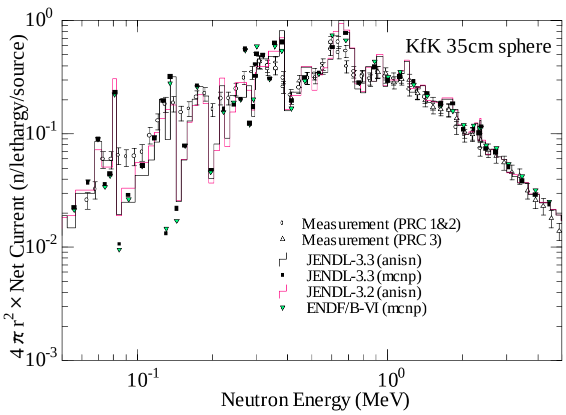

Fig. 4 Results of KfK Iron benchmark.

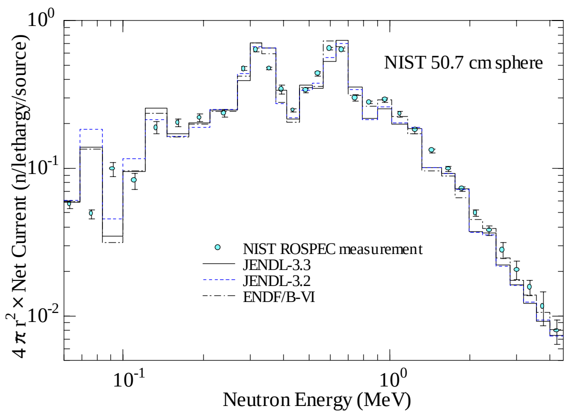

Fig. 5 Results of NIST-ROSPEC Iron benchmark.

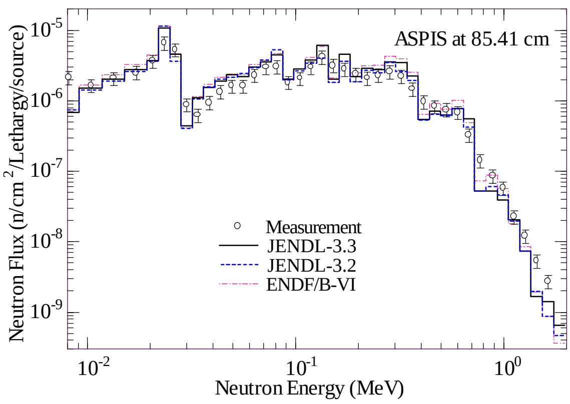

Fig. 6 Results of ASPIS Iron benchmark at 85.41 cm.

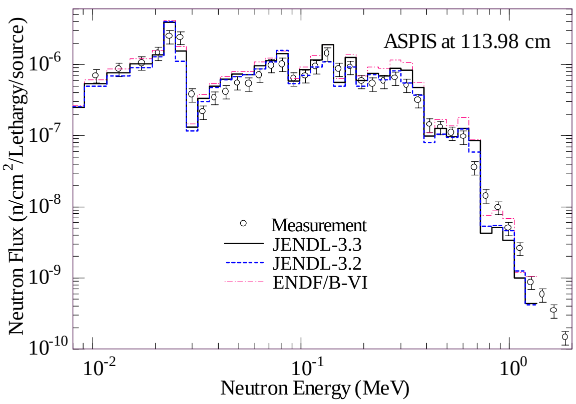

Fig. 7 Results of ASPIS Iron benchmark at 113.98 cm.

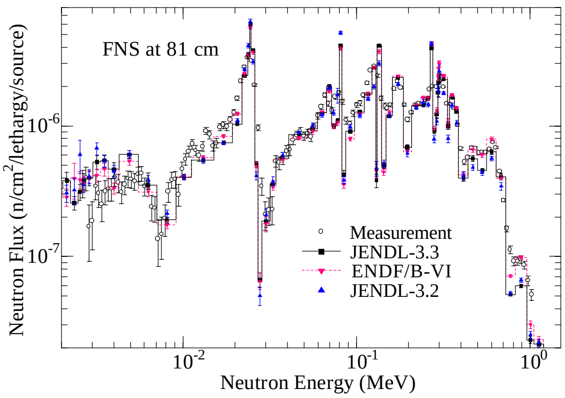

Fig. 8 Results of FNS Iron benchmark at 81 cm.

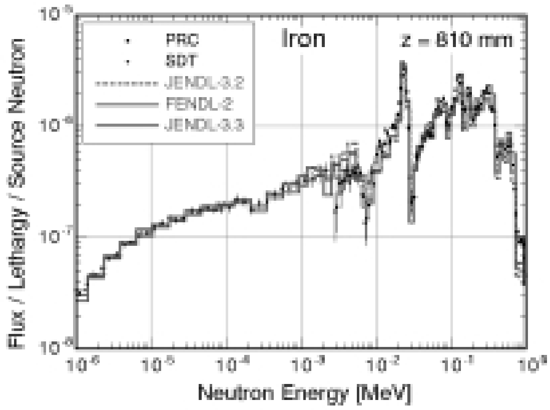

Fig. 9 Results of FNS Iron benchmark at 81 cm.

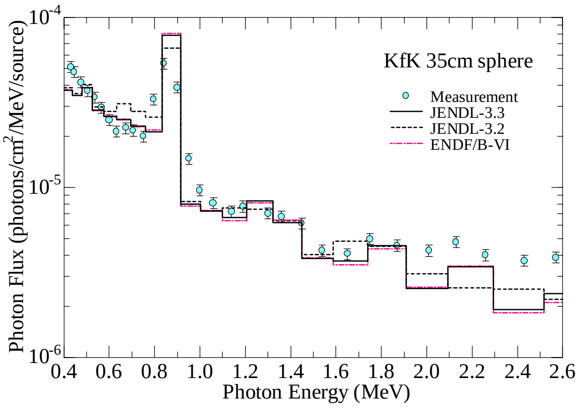

Fig. 10 Results of KfK Iron gamma-ray benchmark.

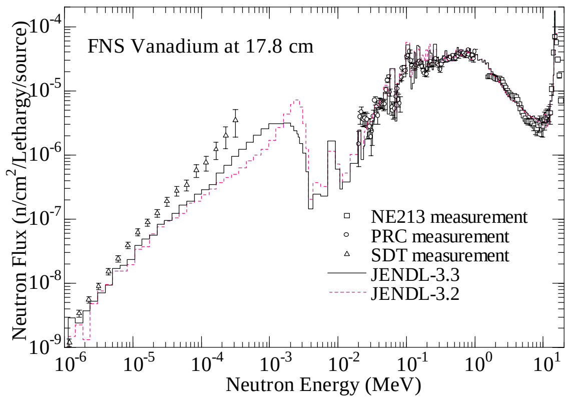

Fig. 13 Results of FNS Vanadium benchmark.

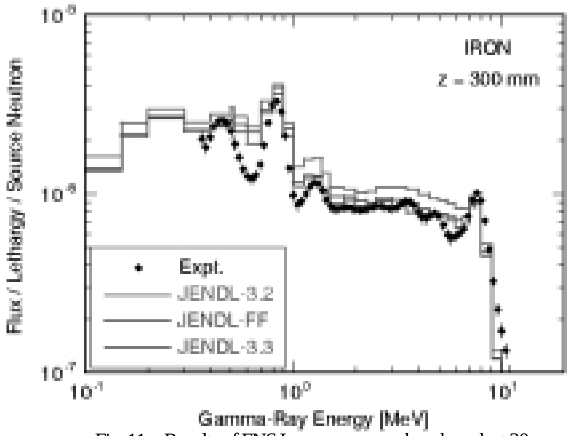

Fig. 11 Results of FNS Iron gamma-ray benchmark at 30 cm.

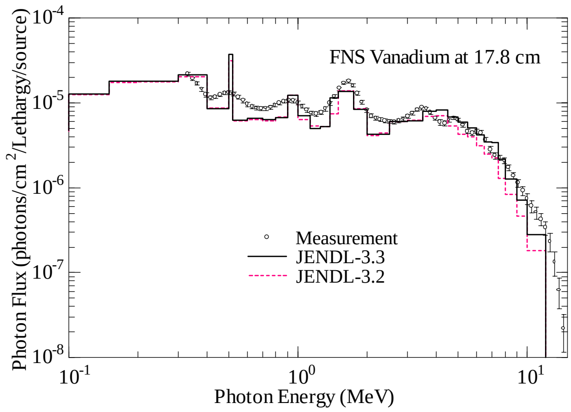

Fig. 14 Results of FNS Vanadium gamma-ray benchmark.

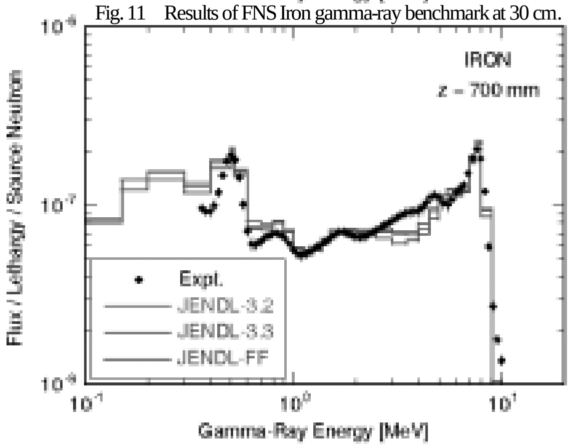

Fig. 12 Results of FNS Iron gamma-ray benchmark at 70 cm.

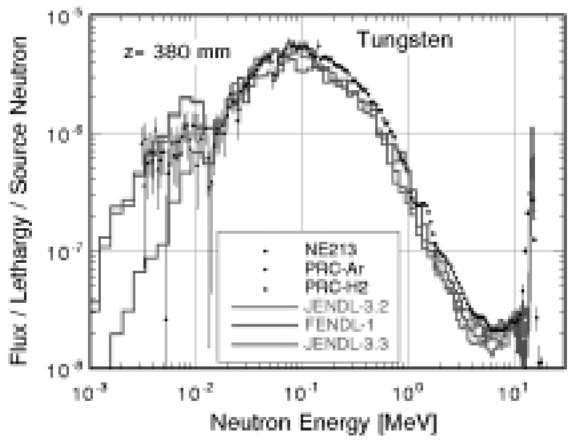

Fig. 15 Results of FNS Tungsten benchmark.

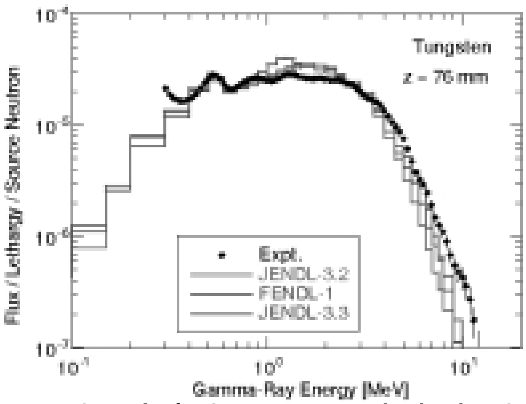

Fig. 16 Results of FNS Tungsten gamma-ray benchmark at 7.6 cm.

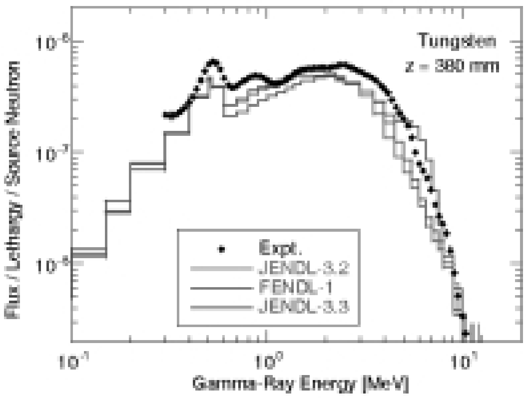

Fig. 17 Results of FNS Tungsten gamma-ray benchmark at 38 cm.

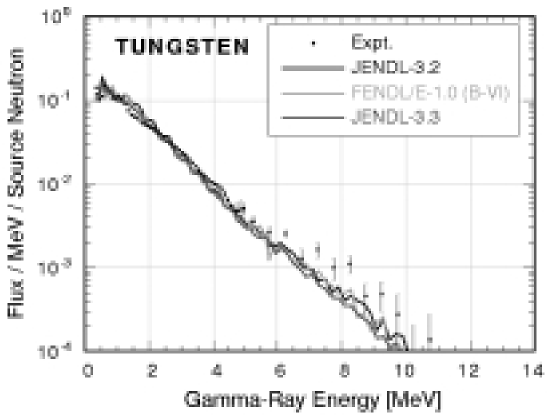

Fig. 18 Results of OKTAVIAN Tungsten gamma-ray benchmark.

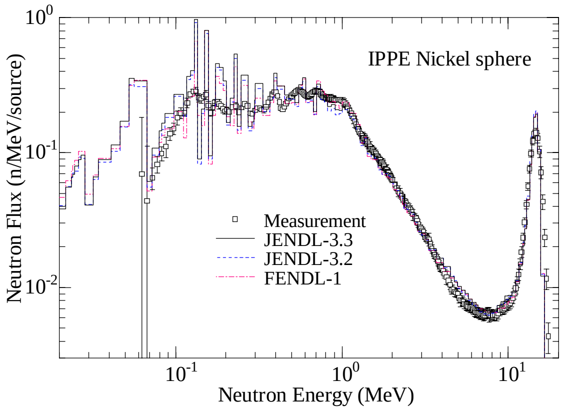

Fig. 19 Results of IPPE Nickel benchmark.

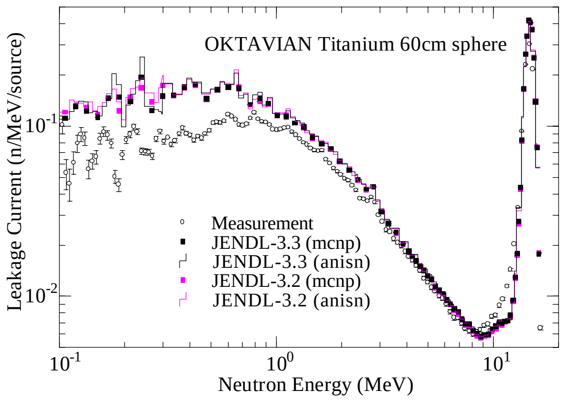

Fig. 20 Results of OKTAVIAN Titanium benchmark.

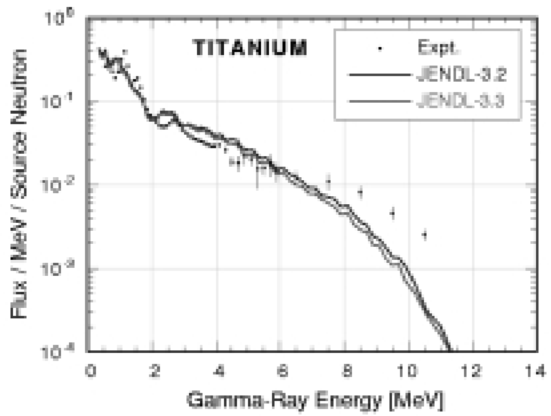

Fig. 21 Results of OKTAVIAN Titanium gamma-ray benchmark.

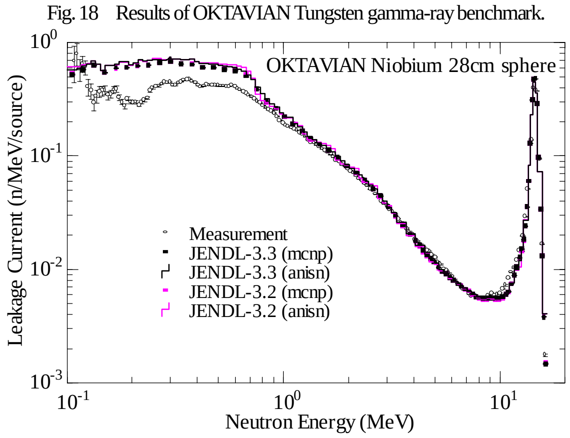

Fig. 22 Results of OKTAVIAN Niobium benchmark.

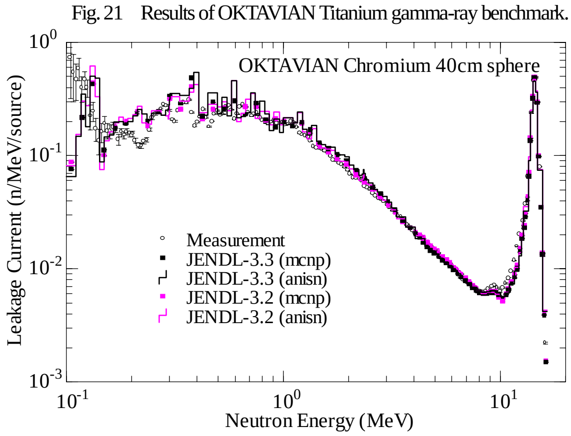

Fig. 23 Results of OKTAVIAN Chromium benchmark.